

Direct mapping of the $\text{CoSi}_2/\text{Si}(111)$ interface by ballistic-electron-emission microscopy and modulation spectroscopy

E. Y. Lee, H. Sirringhaus, and H. von Känel

Laboratorium für Festkörperphysik, Eidgenössische Technische Hochschule Zürich, CH-8093 Zürich, Switzerland

(Received 15 August 1994)

To map the interfacial structure of $\text{CoSi}_2/\text{Si}(111)$, the atomic thickness variations of epitaxial CoSi_2 films were spatially resolved and determined using ballistic-electron-emission microscopy. Modulation spectroscopy was also used, and it showed not only thickness variations, but also strong lateral variations near the interfacial steps and dislocations. Also, a strong energy dependence of the quantum-size effects due to the transition from bound quantized subbands to resonances in CoSi_2 was seen.

The determination of the structures of buried interfaces is important in understanding the properties of thin films as well as their growth. For $\text{CoSi}_2/\text{Si}(111)$, interfacial atomic structure was shown to determine interfacial electronic properties¹ and interfacial step and dislocation structures.² The characterization of the interfacial structures of thin films is also important for understanding many issues of thin-film growth such as strain relaxation, effect of substrate misorientation on film structure, and uniformity of film thickness.

For high lateral resolution of interfacial structures, there exists many useful techniques such as transmission-electron microscopy (TEM),³ scanning-tunneling luminescence microscopy,⁴ ballistic-electron-emission microscopy (BEEM),⁵ and modulation spectroscopy (MS).^{6,7} We report in this paper direct mapping of the $\text{CoSi}_2/\text{Si}(111)$ interfacial structure using two scanning-probe methods. The obtained maps showing interfacial steps, misfit dislocations, and surface steps are consistent with a structural model developed earlier by our group.⁸ The mapping of the interfacial steps was done using BEEM, in which a scanning tunnel microscope (STM) tip injects electrons into a metal overlayer. (The overlayer is made thin enough so that a significant fraction of the injected electrons travel across it to be collected in the substrate as the BEEM current.)⁵

MS was also done and found to give results consistent with BEEM. In addition, near interfacial steps, a strong lateral variation of quantum-size effects (QSE's) was observed by MS. Also, a strong energy dependence of QSE's was observed, consistent with a consideration of the band structure of Si. In MS, surface conductivity is measured by the STM tip by modulating the tip bias voltage at a rate faster than the response of the tunnel-current-feedback loop.^{6,7}

Our samples were grown using a commercial molecular-beam epitaxy (MBE) system for 3-in. wafers. The MBE chamber was connected to a STM chamber, and a custom-built STM was used to investigate the samples grown by MBE in UHV. Our study was *in situ*, and all the STM measurements were done at 77 K. The details of the microscope were published earlier.⁹ Using MBE, the CoSi_2 films were grown by stoichiometric coevaporation of Co and Si onto 7×7 reconstructed Si(111), and annealed at 600 °C for 2–10 min. The samples used for this study had thicknesses of 22, 30, and 35 Å. Previously, samples were grown with the same

recipe and extensively characterized by TEM and by STM,¹⁰ and found to be pinhole-free and consisting of atomically smooth interfacial regions of type-B CoSi_2 on Si bounded by misfit dislocations, which arose because of the -1.2% lattice mismatch (at 300 K) between CoSi_2 and Si. The thin films did *not* have any grain boundaries, being single crystalline.

Figure 1(a) shows an empty-state image of a $2000 \times 1500\text{-Å}^2$ area of the surface of a 22-Å-thick CoSi_2 film

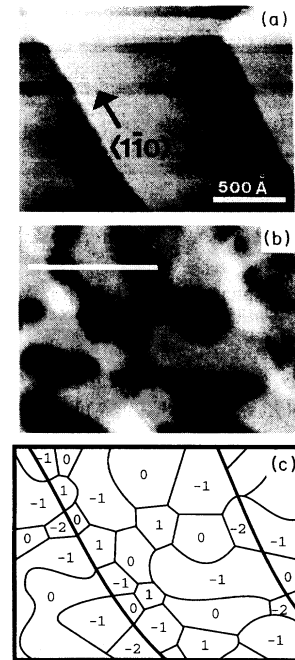


FIG. 1. (a) An empty-state image of a $2000 \times 1500\text{-Å}^2$ area of a 22-Å-thick CoSi_2 film on Si(111) showing two monolayer steps running parallel to $\langle 110 \rangle$ and many dislocations. The tunnel current was 2 nA and the tip voltage was -6 V. (b) A simultaneously acquired BEEM image showing a nearly discrete contrast corresponding exactly to discrete thicknesses of the film. The gray scale ranges from 200 to 400 pA (per nA tunnel current). The white line is explained in Fig. 3. (c) An interfacial map of the same region, the numbers indicating thicknesses (1, 0, -1 , and -2 denote 28, 25, 22, and 19 Å), the solid lines indicating dislocations, and the thicker solid lines indicating surface steps.

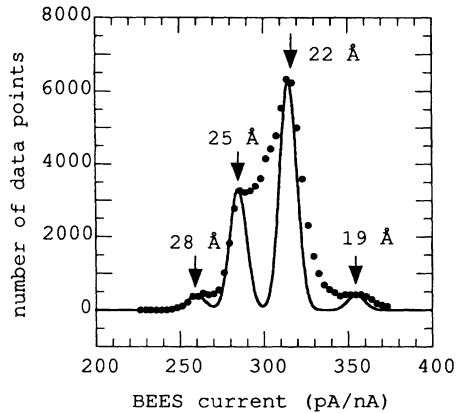


FIG. 2. A histogram of 75 000 data points from a $5000 \times 1500\text{-}\text{\AA}^2$ region, a part of which was shown in Fig. 1. Peaks corresponding to discrete thicknesses of the film are pointed to by arrows. Also shown is a sum of four Gaussian functions, each centered at a peak and having a width approximately equal to that of the noise in the BEEM current (~ 7 pA/nA). Many data points lie between the peaks, and this is because of secondary electrons that lower the spatial resolution of BEEM.

grown on *n*-type Si(111), taken at a tip voltage of -6 V and with a tunnel current of 2 nA. The reader may note two monolayer steps (3.1 Å high) running parallel to $\langle 1\bar{1}0 \rangle$ and the protrusions (~ 0.5 Å high) due to strain fields surrounding misfit dislocations. The protrusions mostly appear as a network of faint and light lines directed in the three equivalent $\langle 1\bar{1}0 \rangle$ directions. The STM observation of misfit dislocations in CoSi_2 has been reported in detail previously by our group, and an interfacial structural model was suggested.⁸ Recently we have also observed the dislocations by BEEM (Ref. 11) and also by current-imaging-tunneling spectroscopy.¹² Figure 1(b) is a simultaneously taken BEEM image. It is striking that the contrasts in the BEEM image are nearly discrete. Regions of different contrasts *always* occur at surface steps or misfit dislocations. Previously, the energy-dependent attenuation length of electrons in CoSi_2 was measured by BEEM and found to be ~ 60 Å at 1 eV above Fermi level and to decrease monotonically with energy.¹³ The nearly discrete contrasts in Fig. 1(b) are due to the dependence of the BEEM current on the local thickness of the film.

In Fig. 2 is shown a histogram of the BEEM current distribution using all data points (75 000 points) from a $5000 \times 1500\text{-}\text{\AA}^2$ area containing the region shown in Fig. 1. Four peaks can be seen at 260, 285, 315, and 355 pA. Also shown is a sum of four Gaussian functions, each being centered over a peak. The standard deviation of each Gaussian function is 7 pA/nA, which was approximately the same as the noise in our BEEM current for that sample. Since the average thickness of the CoSi_2 film was ~ 22 Å, the largest peak at 315 pA in Fig. 2 should correspond to 22 Å (aside from a systematic error of ± 1 ML), and the other peaks to 28, 25, and 19 Å (1 ML being 3.1 Å). Other data sets taken at different locations also give peaks at the same BEEM currents, and also show similar distributions. Knowing the absolute thicknesses of all the regions in Fig. 1(b), a map of the area was made and it is shown in Fig. 1(c), where dislocations and steps can be seen along with the thickness variations. If

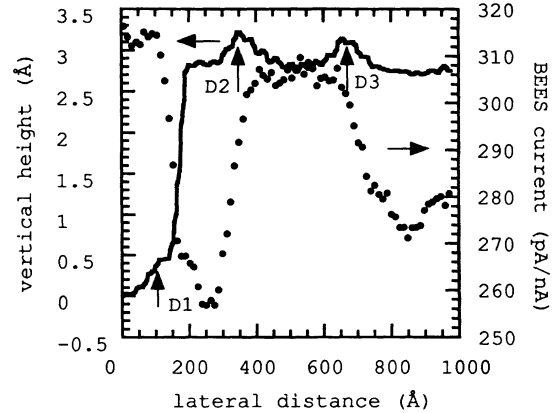


FIG. 3. A line scan from the white line shown in Fig. 1(b). Across the surface step and dislocations, the BEEM currents are close to of 315, 260, 315, and 285 pA, implying that the thicknesses are of 22, 28, 22, and 25 Å. The changes of the BEEM current are seen to be quite broad, occurring over ~ 100 Å, and these show nonballistic transport at -6 V. The data were taken every 10 Å.

one examines the thicknesses, then one can see that they *always* change by only 1 or 2 ML across the dislocations. This is consistent with the current consensus that type-*B* $\text{CoSi}_2/\text{Si}(111)$ interfaces prepared by recipes similar to ours have eightfold-coordinated cobalt atoms everywhere, which force the misfit dislocations (Burgers vector $\mathbf{b} = a/6\langle 11\bar{2} \rangle$) to always couple to interfacial steps.^{2,8}

The network of dislocations in Fig. 1 is seen to be mostly hexagonal, in agreement with the model,⁸ but there also appear regions bounded by four or five regions of different thicknesses. It can also be seen that, in the direction of $\langle 11\bar{2} \rangle$, there are both rising *and* falling single-layer interfacial steps. It is known that monolayer interfacial steps of $\text{CoSi}_2/\text{Si}(111)$ in opposite directions are different, the rising one towards $\langle 11\bar{2} \rangle$ being associated with a 90° partial dislocation and the falling one with a 30° partial dislocation. Therefore, not only can we identify the thicknesses, but we can also identify the specific character of the dislocation.

With regard to the physics of inelastic scattering giving rise to the thickness dependence, let us examine the spatial resolution of BEEM. Figure 3 shows a line scan taken over the white line shown in Fig. 1(b). A topographic profile shows a single monolayer step and three dislocations labeled as *D1*, *D2*, and *D3*. The corresponding BEEM profile shows changes in the BEEM current due to the varying CoSi_2 thickness (values close to 315, 285, and 260 pA are seen, implying that the thicknesses are 22, 25, and 28 Å). The width of the BEEM current profile across the buried steps can define the spatial resolution of BEEM, and it is seen to be ~ 100 Å. Other line profiles show the same order of spatial resolution.

To understand this, let us first consider secondary electrons from electron-electron collisions. It is known that they can contribute to the BEEM current, especially for high biases.¹⁴ Some primary electrons from the tip scatter with electrons in CoSi_2 to create secondary electrons that have broad energy and momentum distribution. The measured BEEM current consists of contributions from both the primary and the secondary electrons. If the fraction of the BEEM current due to the secondary electrons was large, then

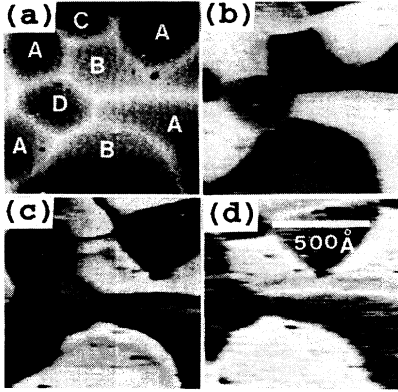


FIG. 4. (a) An empty-state image of a $1000 \times 1000\text{-}\text{\AA}^2$ area of a 30- \AA -thick CoSi_2 film on $\text{Si}(111)$. The tunnel current was 1 nA and the tip voltage was -0.5 V. The gray scale ranges over 1.98 \AA . Dislocations are visible as faint protrusions on the surface. Eight regions are grouped into four classes labeled A, B, C, or D by thickness. (b) A dI/dV image at -0.5 V over the same area (except for thermal drift) showing contrast due to QSE's, which ranges from 2.36 to 4.00 nA/V. Some interfacial steps appear as antinodes (larger dI/dV) and some do not show any relative extremum. Also, wide lateral variation can be seen in the lowest region B. (c) A dI/dV image at -0.75 V showing strong lateral variations of dI/dV near interfacial steps, especially between regions A and B. The gray scale ranges from 0.29 to 1.16 nA/V. (d) A dI/dV image of the same area at -4 V, still showing QSE's. However, the contrast is much weaker than for (b) or (c). The gray scale ranges from 0.68 to 1.41 nA/V.

a worse spatial resolution would be seen. If this is correct, then, at lower energies where fewer secondary electrons are created per primary electron, the spatial resolution should be better. We showed previously (Fig. 2 of Ref. 11) that, at -1.5 V, one does indeed see nanometer resolution at dislocations.

An alternative way of mapping the interfacial structure is to study electron-wave interference in thin films giving rise to QSE's. Recently, this has been done on epitaxial $\text{CoSi}_2/\text{Si}(111)$, and buried interfaces were shown to give rise to changes of the electronic structure that could be detected by STM.^{7,12} For MS, we applied 100-mV modulation at 78 Hz to the tip voltage and the bandwidth of the feedback circuit was narrowed to ~ 50 Hz. The average tunnel current I was constant at 1 nA, and the tip voltage V varied from -0.1 to -4 V. The conductivity dI/dV was measured by a lock-in amplifier.

Figure 4(a) shows an empty state image of a $1000 \times 1000\text{-}\text{\AA}^2$ area of a 30- \AA CoSi_2 over which conductivity images were taken simultaneously with topographic STM images for voltages ranging from -0.25 to -4 V at -0.25 -V intervals. Figures 4(b)–4(d) show three conductivity images taken over approximately the same region for tip voltages of -0.5 , -0.75 , and -4.0 V. The displayed region is flat except for protrusions due to misfit dislocations, and, for the set of images, we kept track of ten regions bounded by dislocations (in some images, only eight or nine regions are visible due to thermal drift). We could group the ten regions into four classes (labeled as A, B, C, and D), each class consisting of regions having the same conductivity for

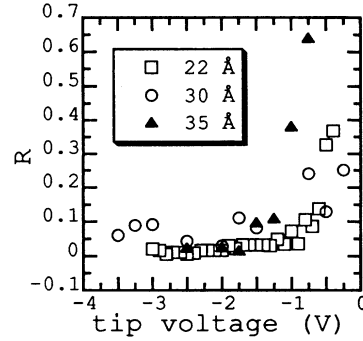


FIG. 5. The normalized conductivity range R , described in the text, is plotted for three samples of thicknesses 22, 30, and 35 \AA . It reflects the strength of the QSE, which is seen to be strongly energy dependent. The energy dependence arises from the fact that, for energies greater than 1.7 eV above the $\text{CoSi}_2/\text{Si}(111)$ Fermi level, the states in CoSi_2 along ΓL are no longer bound by $\text{Si}(111)$ and can only form resonances rather than bound quantized subbands.

all tip voltages within the experimental error. These classes correspond to regions of different thicknesses, in a manner similar to our BEEM result. But, in this case, the exact thicknesses of the classes could not be established; one would need a surface step or a much larger area for that purpose.

From the conductivities of the eight to ten regions at a given voltage, the normalized conductivity range R was calculated, and R was defined to be the standard deviation $\delta(dI/dV)$ of the eight to ten conductivities of the regions normalized by their average value. The quantity R reflects the magnitude of the QSE's, and it was calculated for the data set used in Fig. 4, and also for our other samples. Figure 5 shows R as a function of the tip voltage, and it can be seen to behave similarly for all the samples, decreasing substantially with energy. In fact, except for our 30- \AA sample, for which the CoSi_2 surface-defect density was exceptionally low and the tunnel current was unusually stable, QSE's could not be observed above ~ 1.7 eV. Our observation is consistent with our earlier explanation of this phenomenon, that the quantized subbands in CoSi_2 are no longer confined by Si as the energy exceeds ~ 1.7 eV, so that they can only form resonances rather than true bound states in CoSi_2 .¹² However, we note that QSE's do not completely disappear at high energies, and show Fig. 4(d) to illustrate this point. There, it can be seen that, at -4 V, the contrast due to QSE's still exists, although R is much smaller than at lower energies.

Since the tunnel-current distribution depends on the local density of states (LDOS's) and the BEEM current is directly related to it, QSE's should affect the BEEM current. The observed energy dependence of QSE's implies that, for BEEM on CoSi_2/n -type $\text{Si}(111)$, QSE's should affect the BEEM current mostly at energies below ~ 1.7 eV. This is consistent with our BEEM results.¹¹

It can be seen in Figs. 4(b) and 4(c) that, in addition to the simple change of dI/dV across an interfacial step, there is significant lateral variation away from it. According to a free-electron theory of QSE's,¹⁵ an interfacial step should always give rise to a node in the conductivity ($dI/dV \sim 0$) over itself and to an oscillatory decay in the form of a Bessel function away from it. In most cases, we do see nodes at

interfacial steps [see Fig. 4(c)], but sometimes we see instead either (1) antinode or (2) neither node nor antinode [see Fig. 4(b)]. Furthermore, we do not see oscillatory decay of any kind near the interfacial steps at *any* voltage. There may be three causes of this discrepancy between the theory and experiment. First of all, we have previously shown that, near the Fermi level, the quantized subbands of Λ_3 in CoSi_2 are nearly equally spaced due to its almost linear E - k dispersion relation, which is not very free-electron-like. Second, the measured dI/dV may not accurately reflect the actual LDOS's. Lastly, it seems plausible that the strain field in CoSi_2 causes phase shifts of the electron standing waves and gives rise to the lateral variations. The phase shift of electron waves by strain field surrounding misfit dislocations is routinely observed by plan-view TEM.³ A quantitative calcula-

tion of the phase shifts for our trigonally distorted CoSi_2 films is beyond the scope of this paper.

In conclusion, we have directly mapped the interfacial steps and dislocations by BEEM and by MS. Both techniques are nondestructive *in situ* techniques and give better statistics than cross-sectional TEM. By BEEM, we demonstrated that one can determine the local thickness of a thin film. As the energy of the injected electron is increased, a transition from ballistic transport to a more diffusive transport was observed. Our MS study showed that there is significant lateral variation in QSE's that may be due to strain field in CoSi_2 .

We acknowledge financial support from the Swiss National Science Foundation (NFP 24) and technical assistance from U. Kafader and C. Schwarz.

¹D. R. Hamann, Phys. Rev. Lett. **60**, 313 (1988).

²C. W. T. Bulle-Lieuoma *et al.*, J. Appl. Phys. **73**, 3220 (1993).

³R. Hull *et al.*, Appl. Phys. Lett. **52**, 1605 (1988).

⁴P. Renaud and S. F. Alvarado, Phys. Rev. B **44**, 6340 (1991).

⁵L. D. Bell and W. J. Kaiser, Phys. Rev. Lett. **61**, 2368 (1988).

⁶G. Binnig *et al.*, Phys. Rev. Lett. **55**, 991 (1985).

⁷J. A. Kubby and W. J. Greene, Surf. Sci. Lett. **311**, L696 (1994).

⁸R. Stalder *et al.*, Ultramicroscopy **42**, 781 (1992). The model described in this reference does not take into account the effect of substrate misorientation.

⁹H. Sirringhaus, E. Y. Lee, and H. von Känel, J. Vac. Sci. Technol.

12, 2629 (1994).

¹⁰H. von Känel, Mater. Sci. Rep. **8**, 193 (1992), and references therein.

¹¹H. Sirringhaus, E. Y. Lee, and H. von Känel, Phys. Rev. Lett. **73**, 577 (1994).

¹²E. Y. Lee, H. Sirringhaus, and H. von Känel, Phys. Rev. B **50**, 5807 (1994).

¹³E. Y. Lee, H. Sirringhaus, and H. von Känel, Surf. Sci. Lett. **314**, L823 (1994).

¹⁴L. D. Bell *et al.*, Phys. Rev. Lett. **64**, 2679 (1990).

¹⁵G. Hörmandinger and J. B. Pendry, Surf. Sci. **295**, 34 (1993).

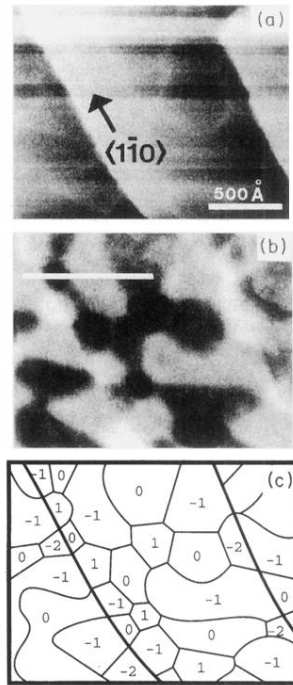


FIG. 1. (a) An empty-state image of a $2000 \times 1500\text{-}\text{\AA}^2$ area of a $22\text{-}\text{\AA}$ -thick CoSi_2 film on $\text{Si}(111)$ showing two monolayer steps running parallel to $\langle 1\bar{1}0 \rangle$ and many dislocations. The tunnel current was 2 nA and the tip voltage was -6 V . (b) A simultaneously acquired BEEM image showing a nearly discrete contrast corresponding exactly to discrete thicknesses of the film. The gray scale ranges from 200 to 400 pA (per nA tunnel current). The white line is explained in Fig. 3. (c) An interfacial map of the same region, the numbers indicating thicknesses (1 , 0 , -1 , and -2 denote 28 , 25 , 22 , and 19 \AA), the solid lines indicating dislocations, and the thicker solid lines indicating surface steps.

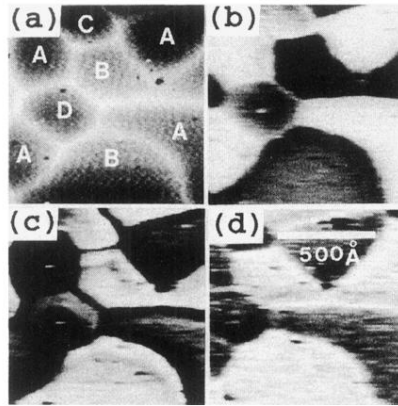


FIG. 4. (a) An empty-state image of a $1000 \times 1000\text{-}\text{\AA}^2$ area of a $30\text{-}\text{\AA}$ -thick CoSi_2 film on $\text{Si}(111)$. The tunnel current was 1 nA and the tip voltage was -0.5 V . The gray scale ranges over 1.98 \AA . Dislocations are visible as faint protrusions on the surface. Eight regions are grouped into four classes labeled A , B , C , or D by thickness. (b) A dI/dV image at -0.5 V over the same area (except for thermal drift) showing contrast due to QSE's, which ranges from 2.36 to 4.00 nA/V . Some interfacial steps appear as antinodes (larger dI/dV) and some do not show any relative extremum. Also, wide lateral variation can be seen in the lowest region B . (c) A dI/dV image at -0.75 V showing strong lateral variations of dI/dV near interfacial steps, especially between regions A and B . The gray scale ranges from 0.29 to 1.16 nA/V . (d) A dI/dV image of the same area at -4 V , still showing QSE's. However, the contrast is much weaker than for (b) or (c). The gray scale ranges from 0.68 to 1.41 nA/V .